Short communication

Electroless copper deposition on a Pt polyfaceted single crystal

J.J. Podestá, J.C. Canullo and A.J. Arvia

Instituto de Investigaciones Fisicoquímicas Teóricas y Aplicadas (INIFTA), Facultad de Ciencias Exactas, Universidad Nacional de La Plata, Sucursal 4, Casilla de Correo 16, (1900) La Plata (Argentina)

A.G. Alvarez

CINDECA, Calle 47 No. 257, (1900) La Plata (Argentina)

Electroless metal deposition involves the simultaneous occurrence of non-conjugated anodic and cathodic reactions at the surface of a substrate immersed in a solution containing a depositing metal ion so that its electroreduction is accompanied by the electro-oxidation of a reducing agent present in the solution. As a typical heterogeneous process, electroless metal deposition implies the transport of reactants, usually the metal ions and the reducing agent, to the substrate surface followed by surface processes such as adsorption/desorption, surface diffusion, and nucleation and growth of new phases [1].

Electroless Cu deposition on Pt by using formaldehyde-containing solutions involves the adsorption of the reducing agent without substrate sensitizing, as the catalytic properties of Pt are sufficient to activate the process. These facts open up the possibility of studying the growth of electrolessly deposited Cu on different faces of polyfaceted single-crystal Pt surfaces through SEM and EDAX techniques, and of attempting to follow the kinetic behaviour of the different crystalline faces of Pt.

The present work is devoted to investigating electroless Cu deposition at regions neighbouring the Pt [100], Pt [110] and Pt [111] poles of polyfaceted microspherical Pt single crystals. The kinetics of this process are already known both in the presence and in the absence of additives in the plating bath [2,3].

Pt polyfaceted single-crystal microspheres of diameter ca. 0.1 cm were prepared by melting the ends of high purity pieces of Pt wires of 0.05 cm OD with either a hydrogen + oxygen flame [4] or a $CH_4 + O_2$ torch [5]. The Pt wire with the microsphere at one end was held in a vertical position by a PTFE holder immersed into the plating solution contained in a glass beaker placed in a thermostat bath.

The electroless Cu plating bath contained 0.032 M $CuSO_4 \cdot 5$ H_2O, 0.054 M EDTA (acid form), 0.20 M formaldehyde (added as 37% by weight solution) and 0.38 M NaOH to obtain pH 12.50.

Electroless Cu deposits were made at 60 °C from a 0.2 l bath without stirring for plating times ranging from 15 to 600 s. The bath was either under H_2 or air saturation at atmospheric pressure.

SEM micrographs of bare and Cu-plated Pt microspheres allowed us to select the different domains around each Pt crystallographic pole and to follow the thickness of the Cu-plated layer through EDAX. The X-ray relative integrated intensity, I_{rel}, of the K_α radiation of the Cu deposit is obtained from the equation

$$I_{rel} = 1.05\rho \, \Delta z = \frac{(I_{Cu})_{K_\alpha}(\text{Cu layer})}{(I_{Cu})_{K_\alpha}(\text{bulk Cu})} \qquad (1)$$

where ρ and Δz are the density and thickness of the Cu deposit, respectively [6,7]. The values of $(I_{Cu})_{K_\alpha}$) for bulk Cu were measured by using a pure Cu microsphere made by melting the end of a Cu wire.

A SEM micrograph of a Cu-plated polyfaceted Pt single-crystal microsphere is shown in Fig. 1A, where the low-index crystalline poles can be identified. The crystallographic features of the Pt microspheres can be enhanced by chemical etching in aqua regia [8]. The locations of low- and some high-index Miller crystalline poles on the Pt (fcc metal lattice) single-crystal microsphere are depicted in Figs. 1B and 1C.

The plot of the amount of electrolessly deposited Cu vs. the plating time (Fig. 2) exhibits at the early stages of the process an induction time for the Pt [111] pole domains, but no induction time for those around Pt [100] and Pt [110]. For the latter, as well as for the Pt [111] pole domains for $t > 200$ s, the amount of electrolessly deposited Cu increases linearly with the plating time with practically the same dQ/dt slope. For the Pt [100] and Pt [110] poles a common straight line going through the origin of the coordinates could probably represent the results reasonably well, after considering the reproducibility and errors involved in the experiments.

The deposited Cu profile run across the Pt [100] pole after 100 s plating illustrates the Cu layer thickness distribution in a surface region around the Pt [100] pole (Fig. 1C). For the sake of clarity, the ranges of the EDAX profiles (Figs. $1C_1$ and $1C_2$) are also indicated in the SEM micrograph (Fig. 1C). The EDAX profiles are slightly distorted because of the proper sphericity of the Pt microsphere.

The above results offer a clear indication that the domains around the Pt [111] poles become less active for the initiation of electroless Cu deposition than those domains located around the Pt [100] and Pt [110] poles.

The overall reaction involves oxidation of the reductant agent formaldehyde to formate [9–14] and reduction of Cu(II) complex ions to Cu(0) at the metal surface. The metal surface acts simultaneously as an anode and a cathode at the mixed potential value [9].
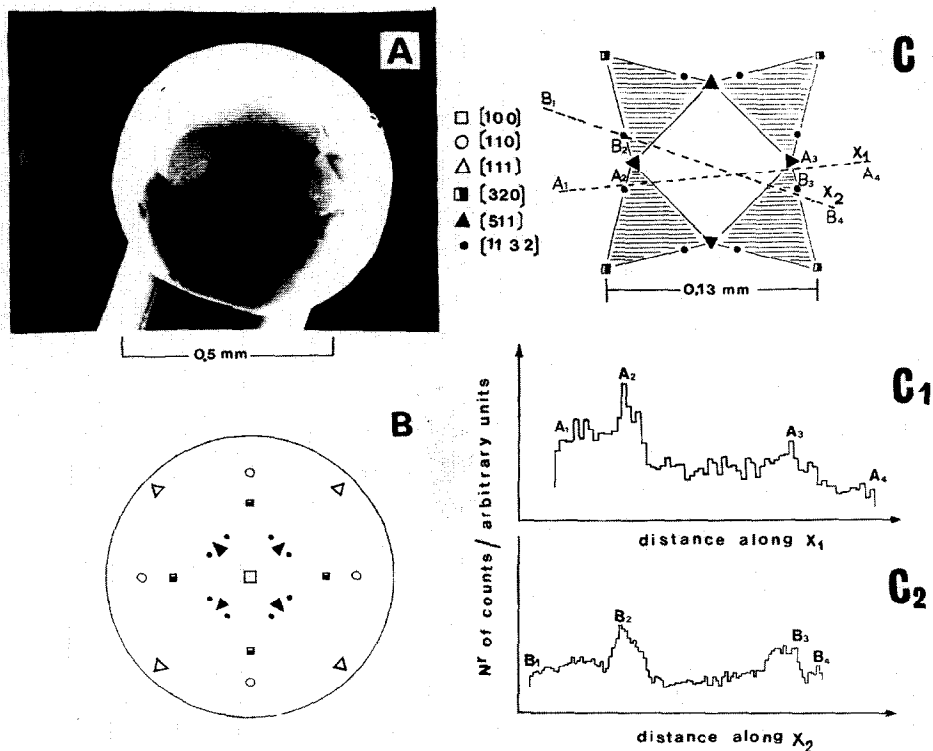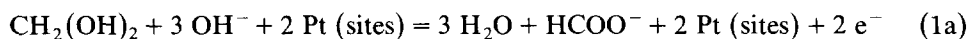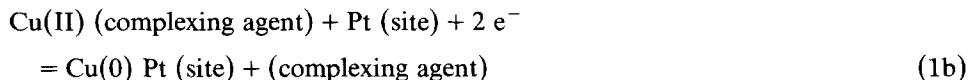
Fig. 1. (A) SEM micrograph of a Pt polyfaceted single-crystal microsphere with electroless Cu plating at 60°C for 100 s. (B) Location of the different crystalline poles formed on the fcc single-crystal hemisphere. (C) Symmetric pattern of electroless Cu developed in the Pt [100] pole direction: (C_1) EDAX results along the X_1 direction; (C_2) EDAX results along the X_2 direction.

The corresponding cathodic reaction can be written as follows [10,11]:

$$CH_2(OH)_2 + 3 \ OH^- + 2 \ Pt \ (sites) = 3 \ H_2O + HCOO^- + 2 \ Pt \ (sites) + 2 \ e^- \qquad (1a)$$

and the cathodic reaction can be expressed as

$$Cu(II) \ (complexing \ agent) + Pt \ (site) + 2 \ e^-$$
$$= Cu(0) \ Pt \ (site) + (complexing \ agent) \qquad (1b)$$

These reactions can explain the influence of the various crystalline faces of Pt on the rate of initiation of Cu deposition. Reaction (1a) involves the formation of two adsorbates, of which at least one, the H-adatom formation, is sensitive to the crystalline face of Pt. For Pt domains around the Pt [111] pole, the adsorption energy of H atoms is lower than that for Pt domains around the Pt [100] pole. For Pt domains around the Pt [111] pole, electroless Cu deposition becomes slower than on the other domains, and in the presence of H_2 in the solution the initiation of the
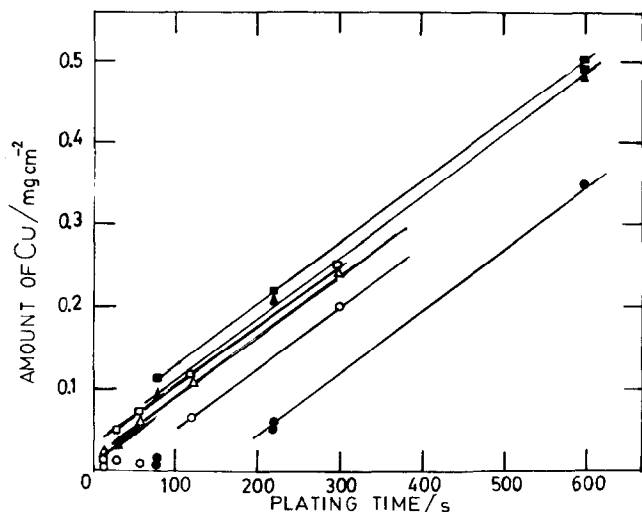
Fig. 2. Amount of electroless Cu plating as a function of the plating time. 60 °C; Pt polyfaceted single-crystal microsphere. (a) Air-saturated solution: (○) [111]; (△) [100]; (□) [110]. (b) Hydrogen-saturated solution: (●) [111]; (▲) [100], (■) [110].

process in regions around the Pt [111] pole becomes even slower. Otherwise, the O_2 dissolved in the solution favours the initiation of Cu deposition.

Electroless Cu deposition on Cu from alkaline formaldehyde–Cu(II)-complex-containing solutions on Cu can be represented by the overall equation [12,13]

$$[Cu(II) \text{ complex}] + 2\ HCHO + 4\ OH^- = Cu(O) + 2\ HCOO^- + 2\ H_2O + H_2$$

$$+ \text{ complexing agent} \qquad (2)$$
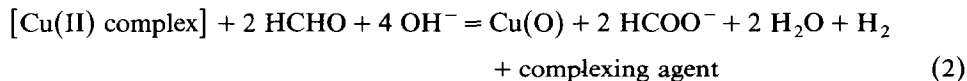
The growth mode of Cu on Cu appears to be largely dependent on the characteristics of the initial deposit.

The greatest reactivity of electroless Cu deposition on a Pt polyfaceted single crystal appears to be associated with portions of the Pt surface initially involving a large density of kinks, corners and terraces.

After complete coverage of the Pt microsphere, the growth of Cu becomes equal to 8×10^{-4} mg Cu s^{-1} cm^{-2} (equivalent to 3.2 μm h^{-1}), a figure which agrees with data reported in the literature for the rate of deposition of polycrystalline Cu [3,14,15].

REFERENCES

1 M. Paunovic and J.Ohno (Eds.), Proc. Symp. Electroless Deposition of Metals and Alloys, Proc. Vol. 88-12, The Electrochemical Society, Pennington, NJ, 1988, p. 3.
2 H. Wiese and K.G. Weil, Ber. Bunsenges. Phys. Chem., 91 (1987) 619.
3 R.C.V. Piatti and J.J. Podestá, Surf. Coatings Technol., 37 (1988) 193.
4 R. Kaischew and B. Mutaftschiew, Z. Phys. Chem., 204 (1955) 334.
5 M. Flytzani-Steptianopoulos, S. Wong and L.D. Schmidt, J. Catal., 49 (1977) 51.
6 S.J.B. Reed, Electron Microprobe Analysis, Cambridge University Press, Cambridge, 1975.
7 G.H. Cockett and C.D. Davis, Br. J. Appl. Phys., 14 (1963) 813.
8 R. Caracciolo and L.D. Schmidt, J. Electrochem. Soc., 130 (1983) 603.
9 M. Paunovic, Plating, 55 (1968) 1161.
10 R.P. Buck and L.R. Griffith, J. Electrochem. Soc., 109 (1962) 1005.
11 R. Schumacher, J.J. Pesek and O.R. Melroy, J. Phys. Chem., 89 (1985) 4338.
12 J.E.A.M. Van den Meerakker, J. Appl. Electrochem., 11 (1981) 387.
13 P. Bindra and J. Roldán, J. Electrochem. Soc., 132 (1985) 2581.
14 R. Sard, J. Electrochem. Soc., 117 (1970) 864.
15 M. Paunovic and C. Stack in R. Weil and R.G. Barradas (Eds.), Electrocrystallization, Softbound Proceeding Series, The Electrochemical Society, Pennington, NJ, 1981, p. 205.